IEEE Access
Multidisciplinary | Rapid Review | Open Access Journal

Received 14 January 2024, accepted 24 January 2024, date of publication 13 February 2024, date of current version 23 February 2024.

Digital Object Identifier 10.1109/ACCESS.2024.3365542

RESEARCH ARTICLE

Observer-Based Adaptive Prescribed-Time H_∞ Coordinated Control for Multiple Robot Manipulators With Prescribed Performance and Input Quantization

WEICHEN LI[1], HAITAO LIU[1,2,3], (Member, IEEE), AND XUEHONG TIAN[1,2]

[1]School of Mechanical Engineering, Guangdong Ocean University, Zhanjiang 524088, China
[2]Shenzhen Institute, Guangdong Ocean University, Shenzhen 518120, China
[3]Guangdong Engineering Technology Research Center of Ocean Equipment and Manufacturing, Zhanjiang 524088, China

Corresponding authors: Haitao Liu (gdliuht@126.com) and Xuehong Tian (gdtianxh@126.com)

This work was supported in part by the Key Project of the Department of Education of Guangdong Province under Grant 2021ZDZX1041 and Grant 2023ZDZX1005, in part by the Shenzhen Science and Technology Program under Grant JCYJ20220530162014033, and in part by the Science and Technology Planning Project of Zhanjiang City under Grant 2021A05023 and Grant 2021E05012.

ABSTRACT In this paper, a prescribed-time adaptive H_∞ cooperative strategy with novel prescribed performance and input quantization based on a leader state observer is proposed for uncertain multiple robot manipulators. First, a novel prescribed performance function is introduced into the asymmetric log-type barrier Lyapunov function, which can limit angle errors and reduce the loss of communication resources among multiple robot manipulators. Second, a new prescribed-time leader state estimation observer is proposed to estimate the leader's state information and pass it to the other followers without acceleration information. Third, a prescribed-time adaptive command filter is designed to solve the ''explosion of the complexity'' problem and improves the convergence performance of the control system. Fourth, an adaptive prescribed-time H_∞ cooperative controller with novel prescribed performance and input quantization is designed. Finally, simulation examples are presented to evaluate the stability of the proposed control system.

INDEX TERMS Prescribed-time H_∞ control, novel prescribed performance, asymmetric log-type barrier Lyapunov function, prescribed-time leader state estimation observer, prescribed-time adaptive command filter, multiple robot manipulators.

I. INTRODUCTION

In recent decades, many methods and techniques have been proposed for consensus tracking control of multiple robot manipulators (RMs). Some of these methods are based on traditional control theories, such as PID control [1] and adaptive control [2], while others utilize modern control theories, such as fuzzy control [3], neural network control [4] and model predictive control [5]. The goal of consensus tracking control is to maintain consistent trajectories and attitudes of multiple RMs while performing tasks. This control method aims to ensure motion coordination between individual manipulators through effective algorithm design and control strategies to achieve efficient and accurate collaborative tasks. In addition, the backstepping technique based on the asymmetric barrier Lyapunov function is also an accessible controller design tool that can cleverly integrate many other advanced algorithms. For example, backstepping has been utilized to address the tracking problem of uncertain RM systems [6] and has also been applied to the consensus tracking control of multiple RMs [7] with the help of adaptive control techniques. Alternatively, a new

The associate editor coordinating the review of this manuscript and approving it for publication was Zhiguang Feng.

performance function is introduced in the asymmetric obstacle Lyapunov function, which limits the trajectory tracking error of multiple RMs to a predefined boundary such that the dynamic response of multiple RMs satisfies the desired control performance. A finite time error tolerance strategy was introduced in [8] for complete state-constrained RMs with a new performance function and time-varying time delay. Fixed-time error tolerance coordinated tracking control based on a novel predefined performance metric was proposed in [9] for dealing with actuator failures, parameter uncertainties and time-varying disturbances in multi-RM systems. In designing a neural network-based prescribed performance control process, the transient performance of an input-saturated robot is improved, and possible boundary spanning problems are mitigated [10]. Although the above studies have successfully addressed the problem of tracking control for multiple RMs, the relationship between the initial design conditions and the actual convergence rate was determined to require additional overshooting constraints. As a result, they are not able to directly determine the time at which the system reaches convergence, and there is still a degree of overshooting. To solve the above problems, the performance function needs to be redesigned, and a new error transformation is introduced to further constrain the boundaries. Based on novel performance functions and error transformations, a predefined-time underwater vehicle control method was presented in [11]. In [12], a novel error transformation method was designed for the design of distributed formation coordinated tracking controllers based on an event-triggered mechanism; this method is capable of maintaining network connectivity and avoiding collisions in purely feedback nonlinear multiagent systems with directional network connectivity.

Most prescribed time consensus control strategies in the past have relied heavily on states such as the angular acceleration information of the leader [13]. However, accurate angular velocity information is obtained relatively easier than accurate angular acceleration states are obtained in some cases, and the angular acceleration information may be disturbed by external perturbations in practice. There is no doubt that inaccurate leader angular acceleration measurements can lead to deterioration of formation control performance [14]. To solve the above problem, a sliding mode controller based on event triggering mechanism and observer was proposed in [15] for delayed systems with unknown disturbances.

Currently, many novel control methods are being designed in the presence of model nonlinear terms and external time-varying disturbances in multi-RM systems with the increasing requirement of control performance. Dynamic surface control is an important controller design tool applied to nonlinear systems with high-order uncertainty and has gained popularity since its widespread application. However, existing backstepping methods are designed to compute the virtual control law differentially, which greatly increases the difficulty of solving the ''complexity explosion'' problem, and the problem becomes increasingly complex to the point of being intractable as the system hierarchy increases. In [16], the problem of singularity and complex explosion is solved by introducing command filters to further compute the derivatives of virtual control functions and reduce the difficulty of derivative computation.

To achieve high-performance multi-RM system tracking control, we cannot ignore nonlinear terms or external environmental disturbances. Therefore, some studies have used neural networks such as self-constructed neural networks and fuzzy neural networks to solve these problems. However, doing so will increase the computational burden. In [17], finite-time H_∞ control techniques were utilized instead of neural networks to address unknown nonlinear terms in the system. However, the initial conditions of the system under the finite time stability theory directly affect the convergence time. To solve this problem, fixed-time H_∞ control methods were introduced in the study so that the given initial conditions no longer determine the convergence time of the system [18]. Nevertheless, the convergence time for fixed-time theory is usually not precise or stable enough. Subsequently, a predefined-time H_∞ control strategy was proposed in [19] to improve the system immunity to unknown disturbances and to reduce the difficulty of system convergence. However, the convergence time for the predefined time theory still suffers from some ambiguity, so we design a prescribed-time H_∞ control method based on the time-scale change strategy. This method aims to achieve a stable state of the system within a prescribed time without being affected by initial conditions.

Inspired by the above research work, an observer-based prescribed-time adaptive H_∞ cooperative controller for the control of multiple RMs is designed in this paper. The controller features novel prescribed performance and input quantization, which can ensure global prescribed time stabilization of multi-RM systems and effectively avoid the ''complexity explosion''. The controller makes important contributions in the following several areas:

(1) A novel prescribed performance metric based on an asymmetric log-type BLF is used to ensure that the steady-state tracking performance of multi-RM systems meets the requirements within a prescribed time. Unlike previous BLFs [20], [21], the prescribed performance is characterized by a fast response speed and good overshoot suppression of the system.

(2) A novel leader state observer design strategy is proposed to approximate and convey leader state information without angular acceleration measurements in the switching communication topology. Unlike the existing research [22], [23], our observer is able to achieve convergence within a prescribed time, which improves the robustness of the control system and speeds up the convergence. The challenge of this problem lies in the complexity of prescribed time convergence.

(3) A prescribed-time adaptive command filter is designed to address the "complexity explosion" problem. Unlike other filters [24], [25], the proposed filter ensures that the filter error converges quickly during the prescribed time. The introduction of the adaptive rate solves the issue of the unknown upper bound ambiguity of the virtual control law derivatives.

(4) Aiming at the problem of aggregate disturbances such as model nonlinear terms and unknown time-varying disturbances, unlike the approximation estimation using radial basis neural networks [26] and fuzzy neural networks [27] in previous studies, a prescribed-time H_∞ formation control strategy is proposed in this paper, which ensures that the initial conditions set by the system are not affecting the convergence speed within the prescribed time. In addition, the system has fast response performance and good robustness when the gain L_2 is also not greater than the given γ.

The remainder of the article is organized as follows. In section II, the model description, graph theory, notations, assumptions and lemmas are presented. In section III, the prescribed-time adaptive cooperative controller is designed. In Section IV and Section V, simulations and conclusions are presented, respectively.

II. PRELIMINARIES

A. MODEL DESCRIPTION

Considering multi-RM systems consisting of a leader RM and N follower RMs, the Euler-Lagrange equation for the *ith* RMs under disturbance is expressed as:

$$M_i\left(q_{i,k}\right)\ddot{q}_{i,k}+C_i\left(q_{i,k},\dot{q}_{i,k}\right)\dot{q}_{i,k}+G_i\left(q_{i,k}\right)=u_{i,k}+\tau_{di} \tag{1}$$

where $q_{i,k},\dot{q}_{i,k},\ddot{q}_{i,k}\in R^n$ denote the joint angle, angular velocity, and angular acceleration of the *ith* follower RMs, respectively. $C_i\left(q_{i,k},\dot{q}_{i,k}\right)\in R^n$ denotes the Coriolis and centrifugal forces. The symmetric positive definite inertia matrix is denoted as $M_i\left(q_{i,k}\right)\in R^{n\times n}$. $G_i\left(q_{i,k}\right)\in R^n$ denotes the force of gravity. $u_{i,k}\in R^n$ is the quantized control input of the *ith* follower RMs, and $\tau_{di}\in R^n$ represents the uncertainty interference torque.

Each RM has the following three characteristics, as shown below:

Characteristic 1: The following parameters $\varphi_{i,1}>0$ and $\varphi_{i,2}>0$ exist such that $0<\varphi_{i,1}\Lambda_{i,k}<M_i(q_{i,k})<\varphi_{i,2}\Lambda_{i,k}$.

Characteristic 2: As shown in $M_i(q_{i,k})\dot{\varpi}_{i,k}+C_i\varpi_{i,k}+G_i(q_{i,k})=\Phi_i(q_{i,k},\dot{q}_{i,k},\varpi_{i,k},\dot{\varpi}_{i,k})\Theta_{i,k}$, where $\varpi_{i,k}$ denotes the differential vector, $\Phi_i(q_{i,k},\dot{q}_{i,k},\varpi_{i,k},\dot{\varpi}_{i,k})$ is the kinetic matrix of regression, and $\Theta_{i,k}$ is the vector of uncertainties.

Characteristic 3: $\dot{M}_i(q_{i,k})-2C_i(q_{i,k},\dot{q}_{i,k})$ is a skew-symmetric matrix.

To satisfy the time-varying effects under the prescribed time control, the time scale change function is as follows:

$$\mu(t)=\begin{cases}\dfrac{T^h}{(T+t_0-t)^h}, & t\in[t_0,t_0+T),\\ 1, & t\in[t_0+T,\infty),\end{cases} \tag{2}$$

where the above two parameters satisfy the designed prescribed time condition: $h>2$, $T>0$.

The derivative of $\mu(t)$ in the interval $t=t_0+T$ is expressed as $\dot{\mu}(t_0+T)$; then,

$$\dot{\mu}(t)=\begin{cases}\dfrac{h}{T}\mu^{1+\frac{1}{h}}, & t\in[t_0,t_0+T),\\ 0, & t\in[t_0+T,\infty).\end{cases} \tag{3}$$

The dynamical equations of the *ith* follower RM are expressed as an uncertain nonlinear second-order system, which is obtained from the differential equation:

$$\begin{cases}\dot{\xi}_{i,k}=\xi_{n,k}\\ \dot{\xi}_{n,k}=f_{\partial i,k}(\xi_{i,k})+vQ(u_{i,k})+\tau_{di}, & i=1,\ldots,N\end{cases} \tag{4}$$

where $\xi_{i,k}\in R^2$ is the state vector for *ith* RMs, $f_{\partial i,k}(\xi_{i,k})\in R$ denotes the uncertainty of the unknown model, $\tau_{di}\in R$ is the external disturbance that varies over time, and $v\in R$ is a known parameter. In addition, the system state variables are not measurable. $Q(u_{i,k})$ must satisfy a quantized input inequality consisting of the design parameters $\lambda_{i,k}$ and $\varepsilon_{i,k}$:

$$\left|Q(u_{i,k})-u_{i,k}\right|\le\lambda_{i,k}\left|u_{i,k}\right|+(1-\lambda_{i,k})\varepsilon_{i,k} \tag{5}$$

The quantizers with boundary constraints include uniform quantizers, logarithmic quantizers, and hysteretic quantizers. The proposed lag quantizer is denoted as follows:

$$Q(u_{i,k})=\begin{cases}u_{ni,k}\mathrm{sgn}(u_{ni,k}), & \dfrac{u_{ni,k}}{1+\lambda_{i,k}}<\left|u_{i,k}\right|\leqslant u_{ni,k}, \quad \dot{u}_{i,k}<0,\\ or\, u_{ni,k}<\left|u_{i,k}\right|\leqslant\dfrac{u_{ni,k}}{1-\lambda_{i,k}}, & \dot{u}_{i,k}>0.\\ u_{ni,k}(1+\lambda_{i,k})\mathrm{sgn}(u_{ni,k}),\\ u_{ni,k}<\left|u_{i,k}\right|\leqslant\dfrac{u_{ni,k}}{1-\lambda_{i,k}}, & \dot{u}_{i,k}<0,\\ or\,\dfrac{u_{ni,k}}{1-\lambda_{i,k}}<\left|u_{i,k}\right|\leqslant\dfrac{u_{ni,k}(1+\lambda_{i,k})}{1-\lambda_{i,k}}, & \dot{u}_{i,k}>0.\\ 0,0<\left|u_{i,k}\right|\leqslant\dfrac{\varepsilon_{i,k}}{1+\lambda_{i,k}}, & \dot{u}_{i,k}<0,\\ or\,\dfrac{\varepsilon_{i,k}}{1+\lambda_{i,k}}<\left|u_{i,k}\right|\leqslant\varepsilon_{i,k}, & \dot{u}_{i,k}>0.\\ Q(u_{i,k}(t^-)), & \dot{u}_{i,k}=0.\end{cases} \tag{6}$$

where $u_{ni,k}=\Delta_{i,k}^{1-\rho_{i,k}}\varepsilon_{i,k}$ satisfies the conditions $n=1,\ldots,12$, $i=1,\ldots,4$, $k=1,2$, $\lambda_{i,k}=\left(1-\Delta_{i,k}\right)/\left(1+\Delta_{i,k}\right)$, and $0<\Delta_{i,k}<1$; then, $Q(u_{i,k})$ exists in the set $H=\{0,\pm u_{ni,k},\pm u_{ni,k}(1+\lambda_{i,k})\}$, with $\varepsilon_{i,k}\in R^+$ standing for the dead zone. A map of $Q(u_{i,k})$ is shown in Fig. 1.

The kinetics of the leader RM are characterized as follows:

$$\begin{cases}\dot{\xi}_{10}=\xi_{20}\\ \dot{\xi}_{20}=u_0(\xi_0,t)\end{cases} \tag{7}$$

where $\xi_0=\left[\xi_{01}\ \xi_{02}\right]^T\in R^m$ is the state vector and $u_0(\xi_0,t)\in R^r$ is the bounded control input for the leader RM.

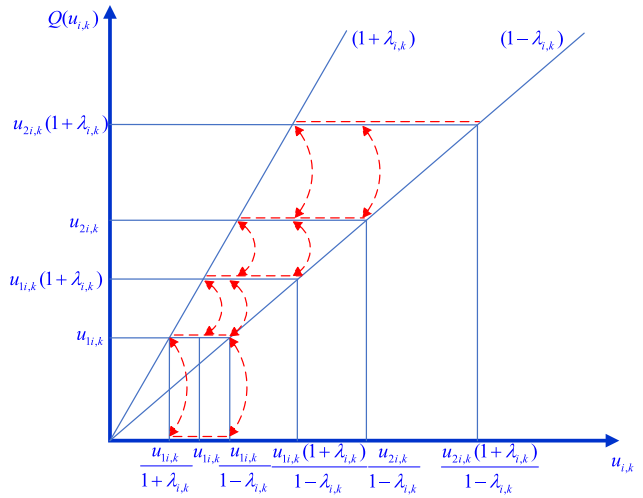

FIGURE 1. The image of the quantized input.

B. GRAPH THEORY DESCRIPTION

Information transfer in the field of multi-RM systems is usually achieved through the use of graph theory with directed and undirected graphs, which are expressed as important theoretical characterizations of unilateral and bilateral information flow between multi-RM systems, respectively. In Graph $G(P, \vartheta)$, $P = [p_1, \ldots, p_N]$ denotes the set of vertices, $\vartheta \in P \times P$ denotes the set of sides (p_i, p_j), and N denotes the number of RMs. The associated adjacency matrix is defined as G for the directed graph $A = [a_{ij}] \in R^{N\times N}$, where $a_{ij} = 1$. $a_{ij} = 1, j \neq i$ indicates that the *ith* follower can receive messages from the *jth* follower; otherwise, $a_{ij} = 0$. The indegree correlation matrix is defined as $E = diag(e_i) \in R^{N\times N}$, where $e_i = \sum_{j\in N_i} a_{ij}$ denotes node i. $L' = E - A$ is defined as the Laplacian matrix. The adjacency matrix of the leader is defined as $A = diag(a_{ij}) \in R^{N\times N}$, where $a_{ij} = 1$ indicates that the leader can connect to the *nth* RM; otherwise, it is defined as $a_{ij} = 0$. Define $b_i = 1$ if the follower can obtain information from the leader; otherwise, it is defined as $b_i = 0$.

C. NOTATIONS

$|*|$ denotes the absolute value. $\arg\min\{*\}$ denotes the minimum value $\{*\}$. $\lceil * \rfloor^q$ represents $|*|^q \operatorname{sign}(*)$. $\|*\|$ represents the Euclidean norm; $\hat{*}$ and $\tilde{*}$ denote the approximation of $*$ and the approximation error, respectively. The sets of real numbers labeled R, R^N and $R^{N\times N}$ represent Euclidean spaces of N increasing dimensions.

D. ASSUMPTIONS AND LEMMAS

Assumption 1: In multi-RM systems with leader and follower roles, there is usually a communication topology graph G that includes one or more leader nodes as well as other nodes as followers. The leader node plays a dominant role in the system and usually has a higher level of intelligence, greater computational power and richer information. On the other hand, the follower nodes act according to the instructions or strategies of the leader nodes.

Assumption 2: The filter input signal β_i is continuous and conductible, and there exists an unknown positive constant θ_i such that the absolute value of the input signal derivative $|\dot{\beta}_i|$ satisfies the condition that does not exceed θ_i.

Lemma 1 [28]: If condition $0 \leq |\gamma| - \gamma \tanh\left(\frac{\gamma}{\delta}\right) \leq w\delta$ is satisfied, then there must exist constants $\delta > 0$ and $\gamma \in R$, where $w = 0.2785$.

Lemma 2 [29]: There exists a Lyapunov function $V(t)$ satisfying

$$\dot{V} \leqslant -\kappa_1 V - \kappa_2 \frac{\dot{\mu}(t)}{\mu(t)} V, \tag{8}$$

where both constants satisfy $\kappa_1 \geq 0, \kappa_2 > 0$ and $\mu(t)$ represented as (2); then, the origin of the system can be globally stabilized within a prescribed time $[t_0, t_0 + T)$. The program is shown as follows:

$$V(t) \leqslant \mu^{-\kappa_2}(t) \mathrm{e}^{-\kappa_1 (t-t_0)} V(t_0), \tag{9}$$

and for the interval $t \in [t_0 + T, +\infty)$, the argument is that $V(t) \equiv 0$.

Lemma 3 [30]: For constant $d > 1$ and $(s-q)^d \leq s^d - q^d$ and for constant $d > 0$ and $q^d(s-q) \leq \frac{1}{1+d}\left(s^{1+d} - q^{1+d}\right)$, the following conditions must be satisfied: $q > 0, s \leq q$.

Lemma 4 [31]: For any performance boundary parameter $\eta(t) > 0$, if there exists a steady-state error E in the compact set $\{\Omega : -\eta(t) < E(t) < \eta(t)\}$, then

$$\ln \frac{\eta^2 e^{E^2}}{\eta^2 - E^2} \leq \left(1 + \frac{1}{\eta^2 - E^2}\right) E^2 \tag{10}$$

Remark 1: The finite-time stabilization settling time is not uniform or predefined. This is because the initial values and other parameters determine the convergence time of the system. However, the predefined time theory allows the initial conditions of the system to no longer affect the stabilization time. In addition, the predefined time stabilization theory [32] allows for fast convergence, and the stabilization time is distributed uniformly and preferentially.

Remark 2: According to the theory of fixed-time stability, the settling time may not be predefined, even if the initial values are the same, because its upper limit is usually limited in some way. Even if the parameters in the fixed-time stability theory can be adjusted so that the system converges in a prescribed time, the parameters may be too large due to an overly conservative estimate of the settling time.

Remark 3: Although the stability of the predefined time stability theory is completely independent of the initial values and other parameters, and the settling time can be predefined, the exact time of convergence is still somewhat unclear. Therefore, a prescribed time control method is designed to solve the above problem and its convergence time is defined in the time scale transformation function, which ensures the stability and predictability of the system.

III. MATH

In this section, a prescribed-time adaptive H_∞ cooperative strategy is introduced for multi-RM systems (MRMSs). First, a novel prescribed performance metric based on an asymmetric log-type BLF is developed, which efficiently adjusts the state convergence performance, improves the stability of the system, and enables the system to achieve optimal performance. Second, a prescribed time state observer is introduced to enable the estimation of the leader angle and angular velocity information without requiring leader angular acceleration. Third, a prescribed-time adaptive command filter is designed to improve the convergence speed while considering the ''complexity explosion''. Fourth, a prescribed time control strategy is introduced to address nonlinear model terms and external disturbances, while a lag quantizer is introduced to avoid the jitter phenomenon. Finally, an observer-based prescribed-time adaptive H_∞ cooperative controller with novel prescribed performance and input quantization is designed, which ensures the overall stability of the system at the prescribed time and improves the robustness of the system.

A. PRESCRIBED-TIME LEADER STATE OBSERVER

In this section, we design a prescribed time cascaded leader state estimation observer that redesigns a new leader for each follower with no corresponding acceleration measurements.

$$\begin{cases} \dot{\hat{x}}_{i,k} = \hat{v}_{i,k} + \kappa_x \left[\sum_{v_j \in N_i} a_{ij} \left(\hat{x}_{j,k} - \hat{x}_{i,k} \right) + b_i \left(x_{0,k} - \hat{x}_{i,k} \right) \right] \\ \qquad + \rho_x \frac{\dot{\mu}}{\mu} \left[\sum_{v_j \in N_i} a_{ij} \left(\hat{x}_{j,k} - \hat{x}_{i,k} \right) + b_i \left(x_{0,k} - \hat{x}_{i,k} \right) \right] \\ \dot{\hat{v}}_{i,k} = \hat{a}_{i,k} + \kappa_v \left[\sum_{v_j \in N_i} a_{ij} \left(\hat{v}_{j,k} - \hat{v}_{i,k} \right) + b_i \left(v_{0,k} - \hat{v}_{i,k} \right) \right] \\ \qquad + \rho_v \frac{\dot{\mu}}{\mu} \left[\sum_{v_j \in N_i} a_{ij} \left(\hat{v}_{j,k} - \hat{v}_{i,k} \right) + b_i \left(v_{0,k} - \hat{v}_{i,k} \right) \right] \\ \dot{\hat{a}}_{i,k} = \kappa_a \left[\sum_{v_j \in N_i} a_{ij} \left(\hat{a}_{j,k} - \hat{a}_{i,k} \right) + b_i \left(z_{a,k} - \hat{a}_{i,k} \right) \right] \\ \qquad + \rho_a \frac{\dot{\mu}}{\mu} \left[\sum_{v_j \in N_i} a_{ij} \left(\hat{a}_{j,k} - \hat{a}_{i,k} \right) + b_i \left(z_{a,k} - \hat{a}_{i,k} \right) \right] \end{cases} \tag{11}$$

where $x_0 = [x_{0,1}, \ldots, x_{0,k}]^T$, $v_0 = [v_{0,1}, \ldots, v_{0,k}]^T$, $a_0 = [a_{0,1}, \ldots, a_{0,k}]^T$ and $i, j = 1, \ldots, 4$, $k = 1, 2$. $z_{a,k}$ is considered an estimate $a_{0,k}$ with direct communication links to the leader when the gain satisfies $\kappa_x, \kappa_v, \kappa_a, \rho_x, \rho_v, \rho_a > u_M$ and the prescribed time observer is shown as follows:

$$\begin{cases} \dot{z}_{x,k} = z_{v,k} - \delta_1 \lceil (z_{x,k} - x_{0,k}) \rfloor - \delta_2 \frac{\dot{\mu}}{\mu} \lceil (z_{x,k} - x_{0,k}) \rfloor \\ \dot{z}_{v,k} = z_{a,k} - \delta_3 \lceil (z_{x,k} - x_{0,k}) \rfloor - \delta_4 \frac{\dot{\mu}}{\mu} \lceil (z_{x,k} - x_{0,k}) \rfloor \\ \dot{z}_{a,k} = -\partial \operatorname{sign} (z_{x,k} - x_{0,k}), z_{a,k}(t_0) = a_{0,k}(t_0), \end{cases} \tag{12}$$

where $\delta_1, \delta_2, \delta_3, \delta_4$ are all positive constants and form a matrix such that $B_1 = \begin{bmatrix} -\delta_1 & 1 \\ -\delta_2 & 0 \end{bmatrix}$ and $B_2 = \begin{bmatrix} -\delta_3 & 1 \\ -\delta_4 & 0 \end{bmatrix}$ satisfy the Hurwitz theorem.

Remark 4: For the *ith* follower that satisfies the requirement $b_i = 0$, the prescribed time observers (11) and (12) must be used because it is not reasonable to set the transfer functions $z_{x,k}$, $z_{v,k}$ and $z_{a,k}$ among the followers. If the transfer functions $z_{a,k}$ are used directly, it is not reasonable for the *jth* follower to satisfy the condition $b_j = 1$, so the state estimation of the leader needs to be reconstructed by the observer (11). The prescribed time observer (12) is used for the *ith* follower that satisfies the condition $b_i = 1$.

Remark 5: Unlike previous fixed-time and finite-time distributed observers in previous work, the PTCLSO consisting of (11) and (12) requires only angular and angular velocity measurements to obtain estimates of the leader states and does not require angular acceleration measurements. Furthermore, it should be noted that the outputs $z_{x,k}$, $z_{v,k}$ and $z_{a,k}$ of observer (12) can be obtained only by a follower that has a direct link with the leader. A direct link with the leader is not available to other followers when $b_i > 0$. Furthermore, if the outputs of observer (12) can be shared between any two followers, the problem of communication link failures would obviously discourage such a communication scheme. Therefore, PTCLSO is practical and robust for reconstructing the state of the leader online without accelerating measurements in many applications.

B. A NOVEL PRESCRIBED PERFORMANCE BASED ON THE BLF

In this section, a new prescribed performance metric based on a log-type BLF is developed, which can be parameterized to constrain the initial overshooting phenomenon of the error, the performance requirements needed for the overall control scheme can be achieved while limiting the angular steady-state error well, and the control system has an overall good robustness and stability.

The angle error of the *ith* follower RM is expressed as follows:

$$e_{xi,k}(t) = \sum_{j=1}^{N} a_{ij}(x_{i,k}(t) - x_{j,k}(t)) + b_i(x_{i,k}(t) - x_{0,k}(t)) \tag{13}$$

The differentiation of (13) is expressed as follows:

$$e_{vi,k}(t) = \sum_{j=1}^{N} a_{ij}(v_{i,k}(t) - v_{j,k}(t)) + b_i(v_{i,k}(t) - v_{0,k}(t)) \tag{14}$$

To achieve the prescribed performance requirements of the system, we designed the following inequality to approximate the angle error $e_{xi,k}(t)$:

$$-\underline{\eta}_{i,k}(t) < e_{xi,k}(t) < \bar{\eta}_{i,k}(t) \tag{15}$$

To ensure that the control system is well constrained by the performance function, the performance function is

represented as follows:

$$\underline{\eta}(t) = \begin{cases} \Upsilon \dfrac{\underline{\eta}_0 - \underline{\eta}_\infty}{\pi} \dfrac{1}{t_f} \sin\left(\dfrac{\pi}{2} - \dfrac{\pi}{2}\dfrac{t}{t_f}\right) & t \in [0, t_f) \\ -\Upsilon(\underline{\eta}_0 - \underline{\eta}_\infty)\left(t - t_f\right) + \rho_\infty, & \\ \underline{\eta}_\infty, & t \in [t_f, \infty) \end{cases} \tag{16}$$

$$\bar{\eta}(t) = \begin{cases} \Upsilon \dfrac{\bar{\eta}_0 - \bar{\eta}_\infty}{\pi} \dfrac{1}{t_f} \sin\left(\dfrac{\pi}{2} - \dfrac{\pi}{2}\dfrac{t}{t_f}\right) & t \in [0, t_f) \\ -\Upsilon(\bar{\eta}_0 - \bar{\eta}_\infty)\left(t - t_f\right) + \bar{\eta}_\infty, & \\ \bar{\eta}_\infty, & t \in [t_f, \infty) \end{cases} \tag{17}$$

The derivative of the performance function is:

$$\dot{\underline{\eta}}(t) = \begin{cases} \Upsilon(\underline{\eta}_0 - \underline{\eta}_\infty)\cos\left(\dfrac{\pi}{2} - \dfrac{\pi}{2}\dfrac{t}{t_f}\right) & t \in [0, t_f) \\ -\Upsilon(\underline{\eta}_0 - \underline{\eta}_\infty), & \\ 0, & t \in [t_f, \infty) \end{cases} \tag{18}$$

$$\dot{\bar{\eta}}(t) = \begin{cases} \Upsilon(\bar{\eta}_0 - \bar{\eta}_\infty)\cos\left(\dfrac{\pi}{2} - \dfrac{\pi}{2}\dfrac{t}{t_f}\right) & t \in [0, t_f) \\ -\Upsilon(\bar{\eta}_0 - \bar{\eta}_\infty), & \\ 0, & t \in [t_f, \infty) \end{cases} \tag{19}$$

To realize the asymmetric performance constraints for multiple RMs, a log-type BLF is constructed as follows [33]:

$$\begin{aligned} V_1 = &\left(1 - q\left(e_{xi,k}\right)\right) \ln\left(\frac{\underline{\eta}_{i,k}^2 e^{e_{xi,k}^2}}{\underline{\eta}_{i,k}^2 - e_{xi,k}^2}\right) \\ &+ q\left(e_{xi,k}\right) \ln\left(\frac{\bar{\eta}_{i,k}^2 e^{e_{xi,k}^2}}{\bar{\eta}_{i,k}^2 - e_{xi,k}^2}\right) \end{aligned} \tag{20}$$

where $q(e_{xi,k})$ is defined as follows:

$$q(e_{xi,k}) = \begin{cases} 1, & e_{xi,k} > 0 \\ 0, & e_{xi,k} \le 0 \end{cases} \tag{21}$$

Remark 6: Unlike in previous research [34], [35], the improved performance function is designed to ensure the angular steady-state error converges within the prescribed time $t_0 + T$. Unlike the conventional prescribed performance [36], the system overshoots while reaching the boundary of the performance envelope, the convergence time of the proposed performance function in this paper is shorter, and the error converges faster when the maximum upper bound is reached while satisfying the same performance requirements.

C. A PRESCRIBED-TIME ADAPTIVE COMMAND FILTER

In this section, a prescribed-time adaptive command filter is designed to alleviate the phenomenon of complex explosions in virtual control rates within a prescribed time.

We design a new error variable $\beta_{ei,k}$ and express the filtering error as follows:

$$\beta_{ei,k} = \beta_{i,k} - \beta_{di,k} \tag{22}$$

where $\beta_{i,k}$ is defined as the signal before filtering and $\beta_{di,k}$ is defined as the signal after filtering. In addition, the initial value satisfies the condition $\beta_{i,k}(0) = \beta_{di,k}(0)$.

Based on assumption 2, we introduce a new state $\hat{\theta}_{i,k}$, which is the estimated value of $\theta_{i,k}$. Let us define the estimated error as follows:

$$\tilde{\theta}_{i,k} = \theta_{i,k} - \hat{\theta}_{i,k} \tag{23}$$

A prescribed-time adaptive command filter is designed as follows:

$$\begin{aligned} \dot{\beta}_{di,k} &= (\kappa_2 + c_2\frac{\dot{\mu}}{\mu})\beta_{ei,k} + \hat{\theta}_{i,k}\tanh\left(\frac{\hat{\theta}_{i,k}\beta_{ei,k}}{\sigma}\right) \\ \dot{\hat{\theta}}_{i,k} &= -(\kappa_3 + c_3\frac{\dot{\mu}}{\mu})\hat{\theta}_{i,k} + \left|\beta_{ei,k}\right| \end{aligned} \tag{24}$$

where σ is a positive constant.

Theorem 1: From assumption 2, it can be observed that there is a boundary constraint limiting the filtering error of the prescribed time adaptive command filter (24) for a prescribed time.

Remark 7: The first-order filter in [37] speeds up convergence, but the convergence rate is related to the gain coefficients. In [38], the command filter achieved system convergence in a fixed time, but it could not approach the unknown upper bound of the virtual control input derivatives. In contrast, the design of the prescribed-time adaptive command filter in this paper is independent of the choice of gain coefficients and ensures that the filtering error is boundary limited and stabilized near zero in the prescribed time. The stability of the system can be improved by designing an adaptive rate method to approximate the uncertain upper bound on the derivative of the virtual control rate.

D. PRESCRIBED-TIME H_∞ CONTROL

The flow of the prescribed time H_∞ controller design is shown below:

For the multi-RM systems:

$$\begin{cases} \dot{x} = f(x) + g(x)q(u) \\ z = h(x) \end{cases} \tag{25}$$

where $x \in R^n$ is the state estimation vector, $q(u) \in R^m$ is the quantized control input vector, $f(x) \in R^r$ is an uncertain perturbation vector, and $z \in R^r$ is a performance characterization vector.

The dynamic compensator is expressed as follows:

$$u = \phi(x, t) \tag{26}$$

This controller is prescribed time stable if it satisfies the following conditions:

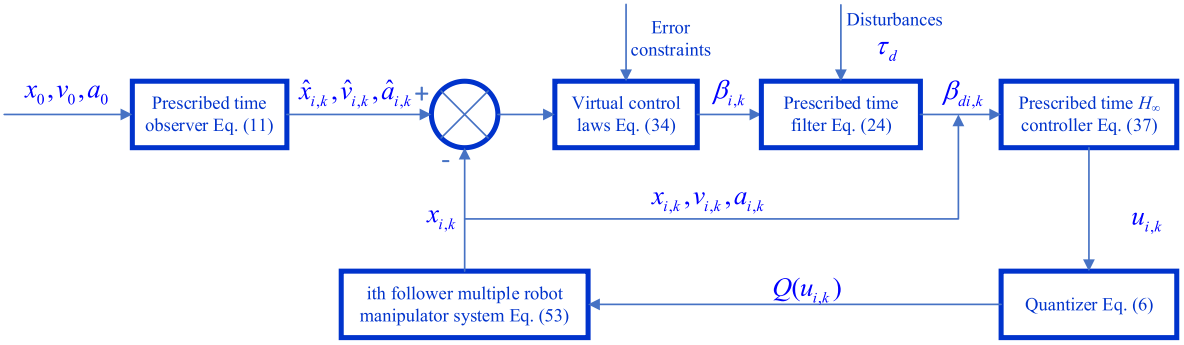

FIGURE 2. Diagram of the multiple robot manipulator formation control strategy.

(1) If the multi-RM systems in (25) and (26) are globally prescribed time stable, then they must satisfy the condition $f(x) = 0$.

(2) Given condition $\gamma > 0$, the system gain L_2 in (25) and (26) does not exceed γ if the output z is generated by $f(x)$ and the initial value $x(t_0) = 0$ satisfies:

$$\int_{t_0}^{t_1} \|z(t)\|^2 dt \le \gamma^2 \int_{t_0}^{t_1} \|f(t)\|^2 dt \tag{27}$$

for all $t_1 > t_0$ and for all uncertain disturbances $f(t)$.

Remark 8: The composite H_∞ controller (26) proposed in this paper is guaranteed to be globally prescribed-time convergent when the gain L_2 satisfies the condition that does not exceed γ, and the prescribed-time controller in (27) should be highly robust. The multi-RM systems are not only prescribed time stable, but also have good immunity to interference.

Remark 9: Unlike the fixed-time or predefined-time H_∞ control strategies mentioned in the past, the prescribed time H_∞ control method is designed to estimate the convergence time more accurately by utilizing novel performance function, quantitative technique and state observer in this paper.

Theorem 2: If there exists a Lyapunov function $V(x)$ in the nonlinear system (25) in a neighborhood $Y \subset R^n$ that satisfies the conditions $B > 0$, $\kappa_1 > 0$ and $\kappa_2 > 0$, then it follows that

(1) $V(x)$ is positive in region Y;

(2) $\dot{V}(x) + \kappa_1 V(x) + \kappa_2 \frac{\dot{\mu}}{\mu} V(x) - B \le \frac{1}{2}(\gamma^2 \|f\|^2 - \|z\|^2)$

If the gain L_2 of the system (25) satisfies the condition that no more than γ or $Y = R^n$ and $V(x)$ are radially unbounded and satisfy the conditions $V(x) \to +\infty$ in case $\|x\| \to +\infty$, the system can subsequently be considered to be partially prescribed time stable at the origin.

Proof:

If the above conditions $f(x) = 0$ are satisfied, inequality 2 in the Theorem 2 can be expressed as follows:

$$\dot{V}(x) + \kappa_1 V(x) + \kappa_2 \frac{\dot{\mu}}{\mu} V(x) - B \le \frac{1}{2}(\gamma^2 \|f\|^2 - \|z\|^2) = -\frac{1}{2}\|z\|^2 \le 0 \tag{28}$$

According to Lemma 1, the multi-RM systems are prescribed time stable.

If the conditions $f(x) \neq 0, V(x) > 0$ are satisfied, inequality 2 in the Theorem 2 can be expressed as follows:

$$\dot{V}(x) \le \dot{V}(x) + \kappa_1 V(x) + \kappa_2 \frac{\dot{\mu}}{\mu} V(x) - B \le \frac{1}{2}(\gamma^2 \|f\|^2 - \|z\|^2) \tag{29}$$

In summary, the system gain L_2 satisfies the condition no more than γ.

The proof is performed.

E. PRESCRIBED-TIME ADAPTIVE COMMAND FILTERED H_∞ CONTROLLER BASED ON A NOVEL PRESCRIBED PERFORMANCE

The derivative of V_1 yields

$$\begin{aligned}\dot{V}_1 = &\left(1 - q\left(e_{xi,k}\right)\right) \\ &\left[\frac{\dot{\underline{\eta}}_{i,k}}{\underline{\eta}_{i,k}} - \frac{\underline{\eta}_{i,k}\dot{\underline{\eta}}_{i,k}}{\underline{\eta}_{i,k}^2 - e_{xi,k}^2} + \left(1 + \frac{1}{\underline{\eta}_{i,k}^2 - e_{xi,k}^2}\right) e_{xi,k}\dot{e}_{xi,k}\right] \\ &+ q\left(e_{xi,k}\right) \\ &\left[\frac{\dot{\bar{\eta}}_{i,k}}{\bar{\eta}_{i,k}} - \frac{\bar{\eta}_{i,k}\dot{\bar{\eta}}_{i,k}}{\bar{\eta}_{i,k}^2 - e_{xi,k}^2} + \left(1 + \frac{1}{\bar{\eta}_{i,k}^2 - e_{xi,k}^2}\right) e_{xi,k}\dot{e}_{xi,k}\right]\end{aligned} \tag{30}$$

The following error variables are introduced in the virtual controller:

$$z_{i,k} = e_{vi,k} - \beta_{i,k} \tag{31}$$

Substituting z_i into (13) and (14), we obtain the following equation:

$$\begin{aligned}\dot{e}_{xi,k} &= z_{i,k} + \beta_{i,k} \\ \dot{z}_{i,k} &= M_{i,k}^{-1} u_{i,k} \left(\sum_{j \in F} a_{ij} + b_i\right) + f_{i,k} \\ &\quad - \left(\sum_{j \in F} a_{ij}\dot{v}_{j,k} + b_i \dot{v}_{0,k}\right) - \dot{\beta}_{i,k}\end{aligned} \tag{32}$$

Then, by substituting (32) into (30), further development can yield

$$\dot{V}_1 = \left(1 - q\left(e_{xi,k}\right)\right)\left(\frac{\dot{\underline{\eta}}_{i,k}}{\underline{\eta}_{i,k}} - \frac{\underline{\eta}_{i,k}\dot{\underline{\eta}}_{i,k}}{\underline{\eta}_{i,k}^2 - e_{xi,k}^2}\right)$$

$$+ q\left(e_{xi,k}\right)\left(\frac{\dot{\bar{\eta}}_{i,k}}{\bar{\eta}_{i,k}} - \frac{\bar{\eta}_{i,k}\dot{\bar{\eta}}_{i,k}}{\bar{\eta}_{i,k}^2 - e_{xi,k}^2}\right)$$
$$+ \left[\left(1 - q\left(e_{xi,k}\right)\right)\left(1 + \frac{1}{\underline{\eta}_{i,k}^2 - e_{xi,k}^2}\right)\right.$$
$$\left. + q\left(e_{xi,k}\right)\left(1 + \frac{1}{\bar{\eta}_{i,k}^2 - e_{xi,k}^2}\right)\right]$$
$$e_{xi,k}(z_{i,k} + \beta_{i,k}) \tag{33}$$

Therefore, the design process of the virtual controller $\beta_{i,k}$ is designed to ensure that the angle error $e_{xi,k}$ converges to the zero-value attachment within the prescribed time:

$$\beta_{i,k} = \left(1 - q\left(e_{xi,k}\right)\right)\left(-p_0\Lambda_{li,k}^{-1}e_{xi,k} - (\kappa_1 + c_1\frac{\dot{\mu}}{\mu})\, e_{xi,k}\right.$$
$$\left. - e_{xi,k}^{-1}\Lambda_{li,k}^{-1}\left(\frac{\dot{\underline{\eta}}_{i,k}}{\underline{\eta}_{i,k}} - \frac{\underline{\eta}_{i,k}\dot{\underline{\eta}}_{i,k}}{\underline{\eta}_{i,k}^2 - e_{xi,k}^2}\right)\right)$$
$$+ q\left(e_{xi,k}\right)\left(-p_0\Lambda_{ui,k}^{-1}e_{xi,k} - (\kappa_1 + c_1\frac{\dot{\mu}}{\mu})e_{xi,k}\right.$$
$$\left. - e_{xi,k}^{-1}\Lambda_{ui,k}^{-1}\left(\frac{\dot{\bar{\eta}}_{i,k}}{\bar{\eta}_{i,k}} - \frac{\bar{\eta}_{i,k}\dot{\bar{\eta}}_{i,k}}{\bar{\eta}_{i,k}^2 - e_{xi,k}^2}\right)\right) \tag{34}$$

where $0 < r < 1$, $\Lambda_{li,k} = 1 + \frac{1}{\underline{\eta}_{i,k}^2 - e_{xi,k}^2}$, $\Lambda_{ui,k} = 1 + \frac{1}{\bar{\eta}_{i,k}^2 - e_{xi,k}^2}$ and T_c is a positive constant.

Therefore, (32) can be rewritten as follows:

$$\dot{e}_{xi,k} = z_{i,k} + \beta_{di,k}$$
$$\dot{z}_{i,k} = M_{i,k}^{-1}u_{i,k}\left(\sum_{j\in F} a_{ij} + b_i\right) + f_{i,k}$$
$$- \left(\sum_{j\in F} a_{ij}\dot{v}_{j,k} + b_i\dot{v}_{0,k}\right) - \dot{\beta}_{di,k} \tag{35}$$

Considering the following nonlinear dynamic system (35), we introduce a novel performance vector

$$z_{i,k} = \begin{bmatrix} \partial_1 e_{xi,k} \\ \partial_2 e_{xi,k} \end{bmatrix} \tag{36}$$

To achieve error convergence within the prescribed time, the actual controller $u_{i,k}$ is designed as follows:

$$u_{i,k} = M_i\left(\sum_{j\in F} a_{ij} + b_i\right)^{-1}\left(\left(\sum_{j\in F} a_{ij}\dot{v}_{j,k} + b_i\dot{v}_{0,k}\right) + \dot{\beta}_{di,k}\right.$$
$$- \left(\left(1 - q\left(e_{xi,k}\right)\right)\Lambda_{li,k} + q\left(e_{xi,k}\right)\Lambda_{ui,k}\right)e_{xi,k}$$
$$\left. - \left(\frac{1}{2\gamma^2} + \frac{\partial_2^2}{2}\right)z_{i,k} - (\kappa_4 + c_4\frac{\dot{\mu}}{\mu})z_{i,k}\right) \tag{37}$$

where $0 < r < 1$, $T_c > 0$.

Theorem 3: For a particular case of multi-RM systems (4) and (7), the system control rates are as shown in (7) and (37), and conditions $p_0 > \frac{\partial_1^2}{2}$ are satisfied to realize the cooperative control problem taking into account the model nonlinear items and external disturbances to ensure that the whole multi-RM system is stabilized at a prescribed time.

Proof:

Substituting (34) into (33), one has

$$\dot{V}_1 = -p_0 e_{xi,k}^2 + \left(\left(1 - q\left(e_{xi,k}\right)\right)\Lambda_{li,k} + q\left(e_{xi,k}\right)\Lambda_{ui,k}\right)z_{i,k}e_{xi,k}$$
$$- \left(\left(1 - q\left(e_{xi,k}\right)\right)\Lambda_{li,k} + q\left(e_{xi,k}\right)\Lambda_{ui,k}\right)(\kappa_1 + c_1\frac{\dot{\mu}}{\mu})e_{xi,k}^2 \tag{38}$$

The following Lyapunov function is selected:

$$V_2 = V_1 + \frac{1}{2}\beta_{ei,k}^2 + \frac{1}{2}\tilde{\theta}_{i,k}^2 \tag{39}$$

Taking the derivative with respect to V_2, one has

$$\dot{V}_2 = \dot{V}_1 + \beta_{ei,k}\dot{\beta}_{ei,k} - \tilde{\theta}_{i,k}\dot{\hat{\theta}}_{i,k} \tag{40}$$

From Lemma 1, by substituting (24) into (40), one has

$$\dot{V}_2 \le -p_0 e_{xi,k}^2 + \left(\left(1 - q\left(e_{xi,k}\right)\right)\Lambda_{li,k} + q\left(e_{xi,k}\right)\Lambda_{ui,k}\right)z_{i,k}e_{xi,k}$$
$$- \left(\left(1 - q\left(e_{xi,k}\right)\right)\Lambda_{li,k} + q\left(e_{xi,k}\right)\Lambda_{ui,k}\right)(\kappa_1 + c_1\frac{\dot{\mu}}{\mu})e_{xi,k}^2$$
$$- (\kappa_2 + c_2\frac{\dot{\mu}}{\mu})\beta_{ei,k} + w\sigma_{i,k} - \tilde{\theta}_{i,k}(\kappa_3 + c_3\frac{\dot{\mu}}{\mu})\hat{\theta}_{i,k} \tag{41}$$

where $w = 0.2785$.

Based on Lemma 3, one has $\tilde{\theta}_{i,k}\hat{\theta}_{i,k} \le (1/2)\left(2\theta_{i,k}^2 - \tilde{\theta}_{i,k}^2\right)$:

$$\dot{V}_2 \le -p_0 e_{xi,k}^2 + \left(\left(1 - q\left(e_{xi,k}\right)\right)\Lambda_{li,k} + q\left(e_{xi,k}\right)\Lambda_{ui,k}\right)z_{i,k}e_{xi,k}$$
$$- \left(\left(1 - q\left(e_{xi,k}\right)\right)\Lambda_{li,k} + q\left(e_{xi,k}\right)\Lambda_{ui,k}\right)(\kappa_1 + c_1\frac{\dot{\mu}}{\mu})e_{xi,k}^2$$
$$- (\kappa_2 + c_2\frac{\dot{\mu}}{\mu})\beta_{ei,k}^2 + w\sigma_{i,k} + \frac{1}{2}(\kappa_3 + c_3\frac{\dot{\mu}}{\mu})(2\theta_{i,k}^2 - \tilde{\theta}_{i,k}^2) \tag{42}$$

Choose a Lyapunov function candidate as

$$V_3 = V_2 + \frac{1}{2}z_{i,k}^2 \tag{43}$$

Taking the time derivative of V_3

$$\dot{V}_3 = \dot{V}_2 + z_{i,k}\dot{z}_{i,k} \le -p_0 e_{xi,k}^2$$
$$+ \left(\left(1 - q\left(e_{xi,k}\right)\right)\Lambda_{li,k} + q\left(e_{xi,k}\right)\Lambda_{ui,k}\right)z_{i,k}e_{xi,k}$$
$$- \left(\left(1 - q\left(e_{xi,k}\right)\right)\Lambda_{li,k} + q\left(e_{xi,k}\right)\Lambda_{ui,k}\right)(\kappa_1 + c_1\frac{\dot{\mu}}{\mu})e_{xi,k}^2$$
$$- (\kappa_2 + c_2\frac{\dot{\mu}}{\mu})\beta_{ei,k}^2 + w\sigma_{i,k} - \frac{1}{2}(\kappa_3 + c_3\frac{\dot{\mu}}{\mu})\tilde{\theta}_{i,k}^2$$
$$+ (\kappa_3 + c_3\frac{\dot{\mu}}{\mu})\theta_{i,k}^2 + z_{i,k}\left(M_{i,k}^{-1}u_{i,k}\left(\sum_{j\in F} a_{ij} + b_i\right)\right.$$
$$\left. + f_{i,k} - \left(\sum_{j\in F} a_{ij}\dot{v}_{j,k} + b_i\dot{v}_{0,k}\right) - \dot{\beta}_{di,k}\right) \tag{44}$$

Substituting (37) into (44), one has

$$\dot{V}_3 \le -\left(\left(1 - q\left(e_{xi,k}\right)\right)\Lambda_{li,k} + q\left(e_{xi,k}\right)\Lambda_{ui,k}\right)$$
$$(\kappa_1 + c_1\frac{\dot{\mu}}{\mu})e_{xi,k}^2 - (\kappa_2 + c_2\frac{\dot{\mu}}{\mu})\beta_{ei,k}^2$$

$$- (\kappa_3 + c_3\frac{\dot{\mu}}{\mu})\tilde{\theta}_{i,k}^2 - (\kappa_4 + c_4\frac{\dot{\mu}}{\mu})z_{i,k}^2 + w\sigma_{i,k} + (\kappa_3 + c_3\frac{\dot{\mu}}{\mu})\theta_{i,k}^2 - p_0 e_{xi,k}^2 - \left(\frac{1}{2\gamma^2} + \frac{\partial_2^2}{2}\right)z_{i,k}^2 + z_{i,k}f_{i,k} \tag{45}$$

According to Lemma 4, we obtain

$$\begin{cases} \left(\ln\frac{\underline{\eta}_{i,k}^2 e^{e_{xi,k}^2}}{\underline{\eta}_{i,k}^2 - e_{xi,k}^2}\right) \le \left(1 + \frac{1}{\underline{\eta}_{i,k} - e_{xi,k}^2}\right)e_{xi,k}^2 \\ \left(\ln\frac{\bar{\eta}_{i,k}^2 e^{e_{xi,k}^2}}{\bar{\eta}_{i,k}^2 - e_{xi,k}^2}\right) \le \left(1 + \frac{1}{\bar{\eta}_{i,k} - e_{xi,k}^2}\right)e_{xi,k}^2 \end{cases} \tag{46}$$

Based on the observation of (46), (45) is further developed as:

$$\begin{aligned} \dot{V}_3 \le & -(\kappa_1 + c_1\frac{\dot{\mu}}{\mu})\left((1 - q\left(e_{xi,k}\right))\ln(\frac{\underline{\eta}_{i,k}^2 e^{e_{xi,k}^2}}{\underline{\eta}_{i,k}^2 - e_{xi,k}^2}) + q\left(e_{xi,k}\right)\ln(\frac{\bar{\eta}_{i,k}^2 e^{e_{xi,k}^2}}{\bar{\eta}_{i,k}^2 - e_{xi,k}^2})\right) - (\kappa_2 + c_2\frac{\dot{\mu}}{\mu})\beta_{ei,k}^2 \\ & - (\kappa_3 + c_3\frac{\dot{\mu}}{\mu})\tilde{\theta}_{i,k}^2 - (\kappa_4 + c_4\frac{\dot{\mu}}{\mu})z_{i,k}^2 + w\sigma_{i,k} - p_0 e_{xi,k}^2 \\ & + (\kappa_3 + c_3\frac{\dot{\mu}}{\mu})\theta_{i,k}^2 - \left(\frac{1}{2\gamma^2} + \frac{\partial_2^2}{2}\right)z_{i,k}^2 + z_{i,k}f_{i,k} \end{aligned} \tag{47}$$

To prove that the L_2 gain of the system satisfies the condition that does not exceed γ, define the function

$$\begin{aligned} H = & \dot{V}_3 + \frac{1}{2}\left(\|z_{i,k}\|^2 - \gamma^2\|f_{i,k}\|^2\right) \\ \le & -(\kappa_1 + c_1\frac{\dot{\mu}}{\mu})\left((1 - q\left(e_{xi,k}\right))\ln(\frac{\underline{\eta}_{i,k}^2 e^{e_{xi,k}^2}}{\underline{\eta}_{i,k}^2 - e_{xi,k}^2}) + q\left(e_{xi,k}\right)\ln(\frac{\bar{\eta}_{i,k}^2 e^{e_{xi,k}^2}}{\bar{\eta}_{i,k}^2 - e_{xi,k}^2})\right) - (\kappa_2 + c_2\frac{\dot{\mu}}{\mu})\beta_{ei,k}^2 \\ & - (\kappa_3 + c_3\frac{\dot{\mu}}{\mu})\tilde{\theta}_{i,k}^2 - (\kappa_4 + c_4\frac{\dot{\mu}}{\mu})z_{i,k}^2 + w\sigma_{i,k} \\ & - p_0 e_{xi,k}^2 + (\kappa_3 + c_3\frac{\dot{\mu}}{\mu})\theta_{i,k}^2 + z_{i,k}f_{i,k} \\ & - \left(\frac{1}{2\gamma^2} + \frac{\partial_2^2}{2}\right)z_{i,k}^2 + \frac{1}{2}\left(\|z_{i,k}\|^2 - \gamma^2\|f_{i,k}\|^2\right) \end{aligned} \tag{48}$$

According to the theory of prescribed-time H_∞ stability and the analytical results of the above equations, (49) can be further derived:

$$\begin{aligned} H \le & -(\kappa_1 + c_1\frac{\dot{\mu}}{\mu})\left((1 - q\left(e_{xi,k}\right))\ln(\frac{\underline{\eta}_{i,k}^2 e^{e_{xi,k}^2}}{\underline{\eta}_{i,k}^2 - e_{xi,k}^2}) + q\left(e_{xi,k}\right)\ln(\frac{\bar{\eta}_{i,k}^2 e^{e_{xi,k}^2}}{\bar{\eta}_{i,k}^2 - e_{xi,k}^2})\right) - (\kappa_2 + c_2\frac{\dot{\mu}}{\mu})\beta_{ei,k}^2 \\ & - (\kappa_3 + c_3\frac{\dot{\mu}}{\mu})\tilde{\theta}_{i,k}^2 - (\kappa_4 + c_4\frac{\dot{\mu}}{\mu})z_{i,k}^2 + w\sigma_{i,k} \\ & - p_0 e_{xi,k}^2 + (\kappa_3 + c_3\frac{\dot{\mu}}{\mu})\theta_{i,k}^2 + \|z_{i,k}\|\,\|f_{i,k}\| \\ & - \left(\frac{1}{2\gamma^2} + \frac{\partial_2^2}{2}\right)z_{i,k}^2 + \frac{\partial_1^2}{2}\|\lambda_{i,k}\|^2 \\ & + \frac{\partial_2^2}{2}z_{i,k}^2 - \frac{\gamma^2}{2}\|f_{i,k}\|^2 \end{aligned} \tag{49}$$

With further consideration of (49) and combining it with the previous derivations, the third step leads to (50) as follows:

$$\begin{aligned} H \le & -(\kappa_1 + c_1\frac{\dot{\mu}}{\mu})\left((1 - q\left(e_{xi,k}\right))\ln(\frac{\underline{\eta}_{i,k}^2 e^{e_{xi,k}^2}}{\underline{\eta}_{i,k}^2 - e_{xi,k}^2}) + q\left(e_{xi}\right)\ln(\frac{\bar{\eta}_{i,k}^2 e^{e_{xi,k}^2}}{\bar{\eta}_{i,k}^2 - e_{xi,k}^2})\right) - (\kappa_2 + c_2\frac{\dot{\mu}}{\mu})\beta_{ei,k}^2 \\ & - (\kappa_3 + c_3\frac{\dot{\mu}}{\mu})\tilde{\theta}_{i,k}^2 - (\kappa_4 + c_4\frac{\dot{\mu}}{\mu})z_{i,k}^2 + w\sigma_{i,k} \\ & - p_0 e_{xi,k}^2 + (\kappa_3 + c_3\frac{\dot{\mu}}{\mu})\theta_{i,k}^2 + \|z_{i,k}\|\,\|f_{i,k}\| \\ & - \frac{1}{2\gamma^2}z_{i,k}^2 + \frac{\partial_1^2}{2}\|\lambda_{i,k}\|^2 - \frac{\gamma^2}{2}\|f_{i,k}\|^2 \end{aligned} \tag{50}$$

Immediately following the derivation of (50) can be equated to

$$\begin{aligned} H = & -(\kappa_1 + c_1\frac{\dot{\mu}}{\mu})\left((1 - q\left(e_{xi,k}\right))\ln(\frac{\underline{\eta}_{i,k}^2 e^{e_{xi,k}^2}}{\underline{\eta}_{i,k}^2 - e_{xi,k}^2}) + q\left(e_{xi,k}\right)\ln(\frac{\bar{\eta}_{i,k}^2 e^{e_{xi,k}^2}}{\bar{\eta}_{i,k}^2 - e_{xi,k}^2})\right) - (\kappa_2 + c_2\frac{\dot{\mu}}{\mu})\beta_{ei,k}^2 \\ & - (\kappa_3 + c_3\frac{\dot{\mu}}{\mu})\tilde{\theta}_{i,k}^2 - (\kappa_4 + c_4\frac{\dot{\mu}}{\mu})z_{i,k}^2 + w\sigma_{i,k} \\ & - p_0 e_{xi,k}^2 + (\kappa_3 + c_3\frac{\dot{\mu}}{\mu})\theta_{i,k}^2 + \frac{\partial_1^2}{2}\|e_{xi,k}\|^2 \\ & - \left(\frac{1}{\sqrt{2}\gamma}z_{i,k} - \frac{\gamma}{\sqrt{2}}f_{i,k}\right)^T\left(\frac{1}{\sqrt{2}\gamma}z_{i,k} - \frac{\gamma}{\sqrt{2}}f_{i,k}\right) \end{aligned} \tag{51}$$

According to Lemma 2, one obtains

$$\begin{aligned} H \le & -(\kappa_1 + c_1\frac{\dot{\mu}}{\mu})\left((1 - q\left(e_{xi,k}\right))\ln(\frac{\underline{\eta}_{i,k}^2 e^{e_{xi,k}^2}}{\underline{\eta}_{i,k}^2 - e_{xi,k}^2}) + q\left(e_{xi,k}\right)\ln(\frac{\bar{\eta}_{i,k}^2 e^{e_{xi,k}^2}}{\bar{\eta}_{i,k}^2 - e_{xi,k}^2})\right) - (\kappa_2 + c_2\frac{\dot{\mu}}{\mu})\beta_{ei,k}^2 \\ & - (\kappa_3 + c_3\frac{\dot{\mu}}{\mu})\tilde{\theta}_{i,k}^2 - (\kappa_4 + c_4\frac{\dot{\mu}}{\mu})z_{i,k}^2 \\ & + B_{i,k} - \left(p_0 - \frac{\partial_1^2}{2}\right)\|e_{xi,k}\|^2 \end{aligned}$$

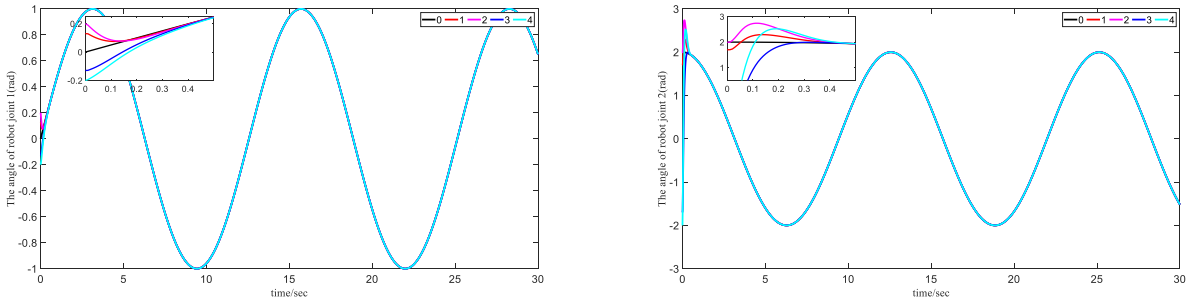

FIGURE 3. Angle tracking effect graph within the prescribed time $t = t_0 + T = 0.5$ s.

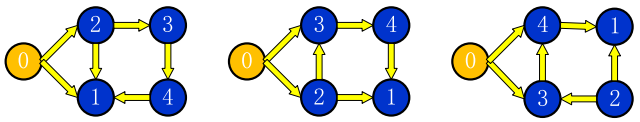

FIGURE 4. The switching-directed topology.

$$\leq -(\kappa_5 + c_5\frac{\dot{\mu}}{\mu})V_3 + B_{i,k} \tag{52}$$

where $B_{i,k} = w\sigma_{i,k} + (\kappa_3 + c_3\frac{\dot{\mu}}{\mu})\theta_{i,k}^2 - \left(p_0 - \frac{\partial_1^2}{2}\right)\|e_{xi,k}\|^2$.

The proof is performed.

Remark 10: According to Lemmas 1-4 and Assumptions 1-2, the derivations of this paper can be written as (52), where the designed controller is shown in Fig. 2.

IV. SIMULATION

To prove the stability of the controller designed in this paper, five dual-joint robots are designed for verification, which consists of one leader RM and four follower RMs. The communication topology is switched every 10s, as shown in Fig. 4.

For this purpose, the two-jointed robot manipulator is shown in Fig. 5 and the dynamical equation is represented by (1), where

$$\begin{bmatrix} M_{i,11} & M_{i,12} \\ M_{i,21} & M_{i,22} \end{bmatrix}\begin{bmatrix} \ddot{q}_{i,1} \\ \ddot{q}_{i,2} \end{bmatrix} + \begin{bmatrix} C_{i,11} & C_{i,12} \\ C_{i,21} & C_{i,22} \end{bmatrix}\begin{bmatrix} \dot{q}_{i,1} \\ \dot{q}_{i,2} \end{bmatrix} + \begin{bmatrix} G_{i,11} \\ G_{i,21} \end{bmatrix} = \begin{bmatrix} Q(u_{i,1}) \\ Q(u_{i,2}) \end{bmatrix} + \begin{bmatrix} \tau_{d1} \\ \tau_{d2} \end{bmatrix} \tag{53}$$

where $M_{i,11} = J_{i,1} + m_{i,2}l_{i,1}^2 + J_{i,2} + 0.25m_{i,2}l_{i,2}^2 + m_{i,2}l_{i,1}l_{i,2}\cos q_{i,2}$, $M_{i,12} = M_{i,21} = J_{i,2} + 0.25m_{i,2}l_{i,2}^2 + 0.5m_{i,2}l_{i,1}l_{i,2}\cos q_{i,2}$, $M_{i,22} = J_{i,2} + 0.25m_{i,2}l_{i,2}^2$, $C_{i,11} = -0.5m_{i,2}l_{i,1}l_{i,2}\dot{q}_{i,2}\sin q_{i,2}$, $C_{i,12} = -0.5m_{i,2}l_{i,1}l_{i,2}\left(\dot{q}_{i,1}+\dot{q}_{i,2}\right)\sin q_{i,2}$, $C_{i,21} = 0.5m_{i,2}l_{i,1}l_{i,2}\dot{q}_{i,1}\sin q_{i,2}$, $C_{i,22} = 0$, $G_{i,11} = (0.5m_{i,1}+m_{i,2})g\cos q_{i,1}+0.5m_{i,2}l_{i,2}g\cos(q_{i,1}+q_{i,2})$, $G_{i,21} = 0.5m_{i,2}l_{i,2}g\cos(q_{i,1}+q_{i,2})$.$q_{i,1}$ and $q_{i,2}$ define the joint angle, and $J_{i,1}$ and $J_{i,2}$ represent the joint torque. $l_{i,1}$ and $l_{i,2}$ represent the length of the link bar. $m_{i,1}$ and $m_{i,2}$ denote the weights of the link bars.

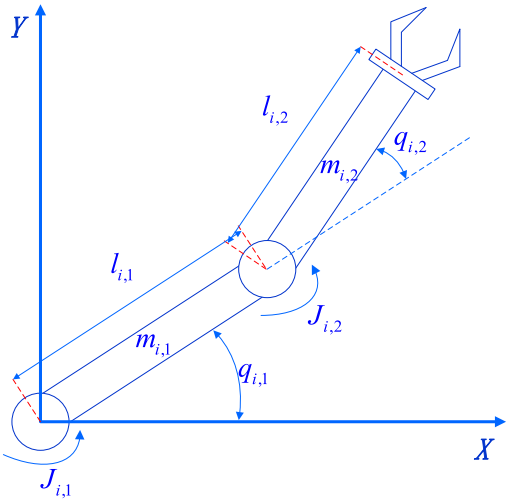

FIGURE 5. A two-joint robot manipulator platform.

TABLE 1. Physical parameters of the robot manipulators.

Symbol	Quantity	Value
$m_{i,1}$	the quality of rod 1	0.96 kg
$m_{i,2}$	the quality of rod 2	1.15 kg
$l_{i,1}$	the length of rod 1	1 m
$l_{i,2}$	the length of rod 2	0.95 m
$J_{i,1}$	the moment of inertia of joint 1	0.21 kg/m2
$J_{i,2}$	the moment of inertia of joint 2	0.4 kg/m2
g	the constant force of gravity	9.81 m/s2

The leader preset trajectories are represented as follows:

$$\begin{cases} s_{d1} = \sin(0.5t) \\ s_{d2} = 2\cos(0.5t) \end{cases} \tag{54}$$

with $x_0 = [s_{d1}, s_{d2}]^T$, $v_0 = [\dot{s}_{d1}, \dot{s}_{d2}]^T$ and $a_0 = [\ddot{s}_{d1}, \ddot{s}_{d2}]^T$.

The disturbances are set as follows:

$$\begin{cases} \tau_{d1} = 1 + 0.5\sin(0.5t) \\ \tau_{d2} = 0.5 + 0.5\cos(0.5t) \end{cases} \tag{55}$$

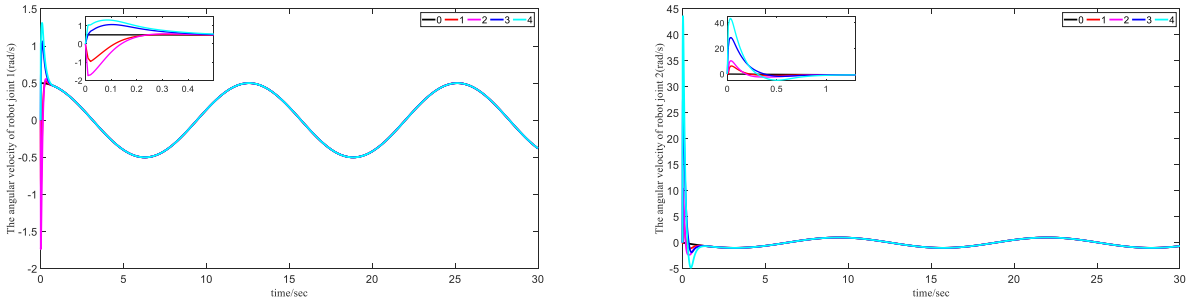

FIGURE 6. Angular velocity tracking effect graph within the prescribed time $t = t_0 + T = 0.5$ s.

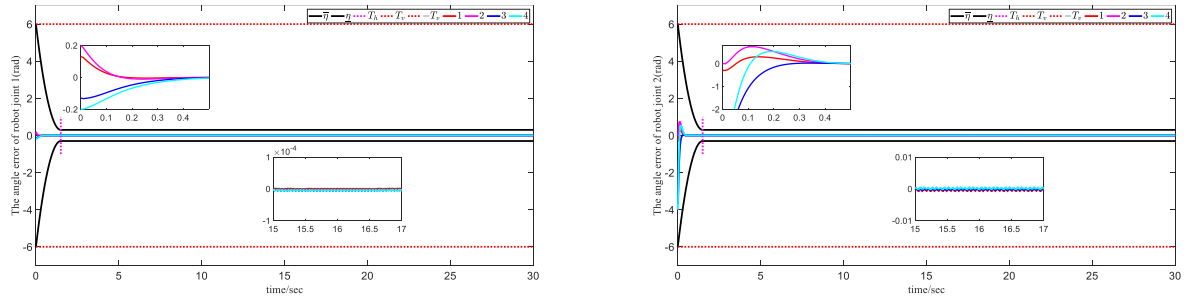

FIGURE 7. Angle tracking error graph within the prescribed time $t = t_0 + T = 0.5$ s.

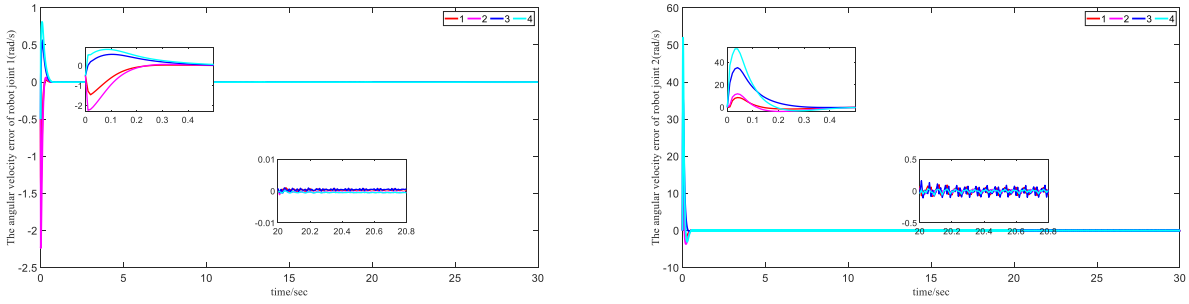

FIGURE 8. Angular velocity tracking error graph within the prescribed time $t = t_0 + T = 0.5$ s.

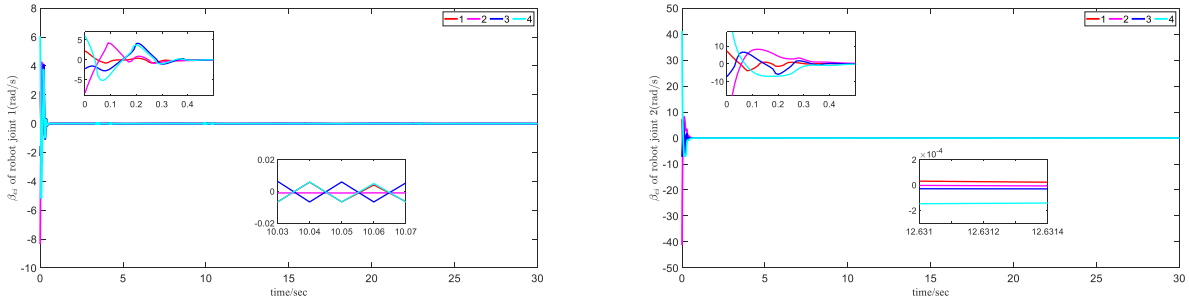

FIGURE 9. Filtering error within the prescribed time $t = t_0 + T = 0.5$ s.

The initial states of the follower robots are $x_{d1}(0) = [0.13, 1.7, 0.2, 2, -0.13, -1.7, -0.2, -2]^T$, $x_{d2} = [0, 0, 0, 0, 0, 0, 0, 0]^T$. The *ith* follower robot manipulator controller u_i is set as follows: $\kappa_1 = 10$, $\kappa_2 = \kappa_3 = 3$, $\kappa_4 = 10$, $\partial_2 = 1$, $\gamma = 1$, and $c_1 = c_2 = c_3 = c_4 = 2$. The settling time is given as $t_0 = 0s$, $T = 0.5s$, and $h = 0.3$. The performance function values are shown as follows: $\eta_0 = 3$, $\bar{\eta}_0 = 3$, $\underline{\eta}_\infty = 1.5$, $\bar{\eta}_\infty = 1.5$, $\Upsilon = 0.8$, and $t_f = 1.5s$. To verify the superiority of the proposed prescribed time H_∞ (PSTH) controller, the parameter settings for the fixed-time H_∞(FXTH) controller

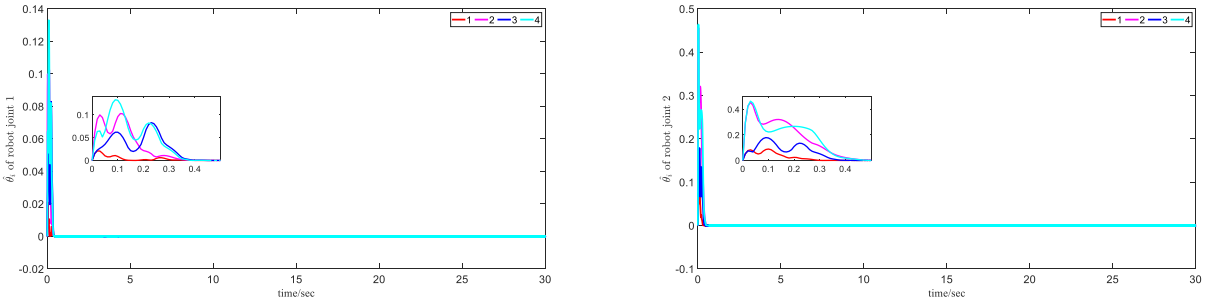

FIGURE 10. The filter adaptive laws.

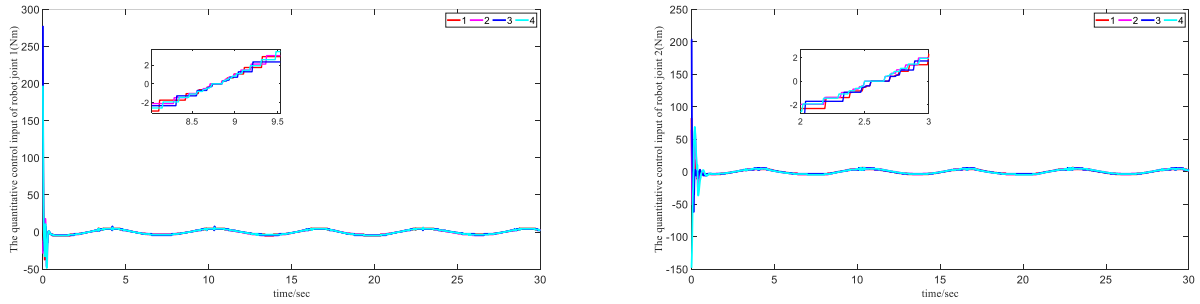

FIGURE 11. Control input graph.

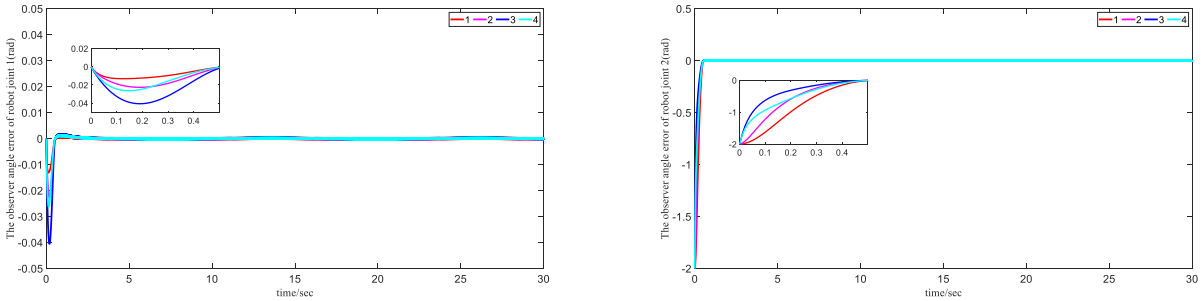

FIGURE 12. Angle errors of the observer within the prescribed time $t = t_0 + T = 0.5$ s.

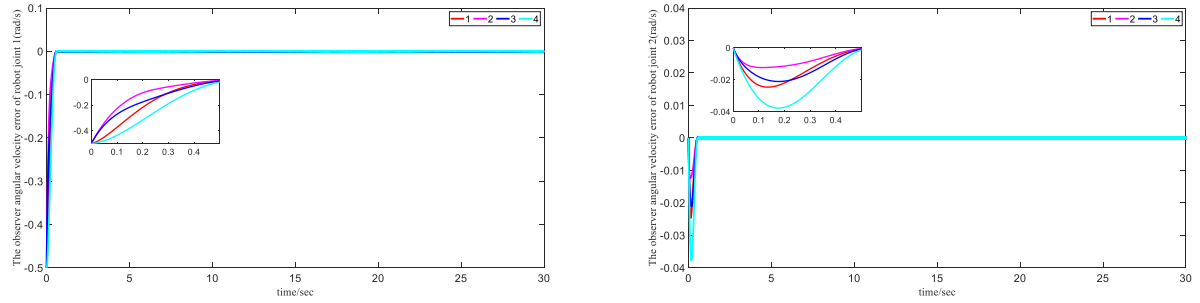

FIGURE 13. Angular velocity errors of the observer within the prescribed time $t = t_0 + T = 0.5$ s.

comparison experiment [18] are: $\alpha = 0.8$, $\beta = 1.2$, $\partial_2 = 1$, $p_1 = p_2 = p_3 = p_4 = 1$, and $\gamma = 1$.

The main use cases for these multiple RMs are welding [39] and painting [40] in industrial production. To simplify the simulation process, the two-degree-of-freedom robotic arm is used. Considering that the problem of limited communication bandwidth for multiple RMs may occur during industrial production, which directly leads to the deterioration of the overall control performance, the input quantization techniques is introduced to improve the situation,

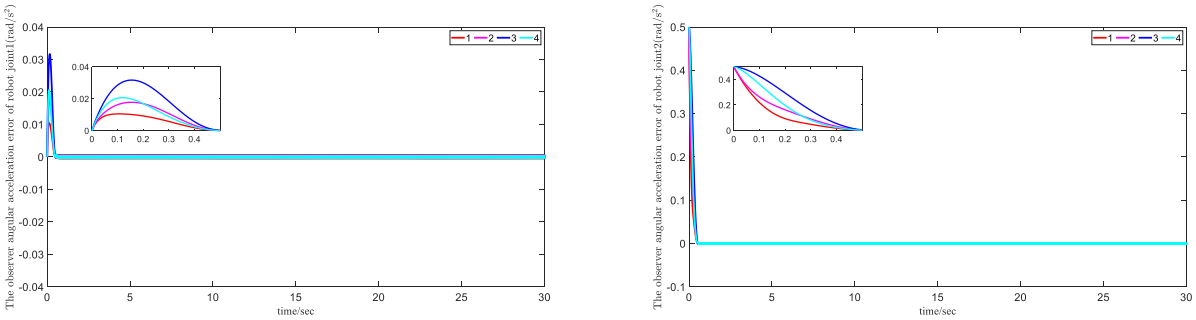

FIGURE 14. Angular acceleration errors of the observer within the prescribed time $t = t_0 + T = 0.5$ s.

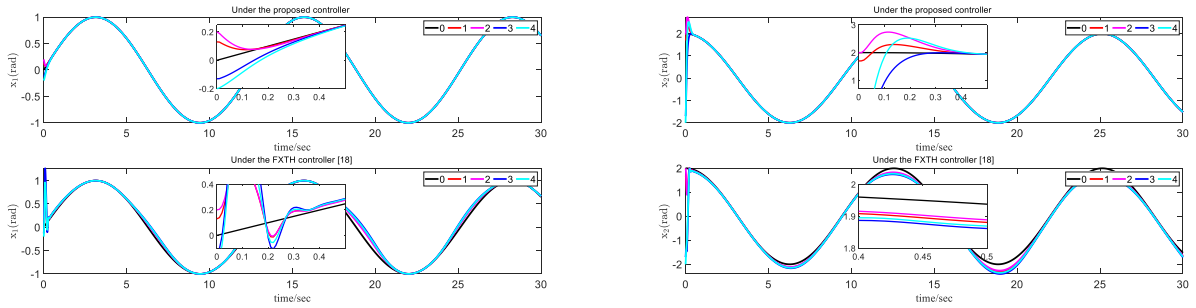

FIGURE 15. Angle tracking effect comparison graph.

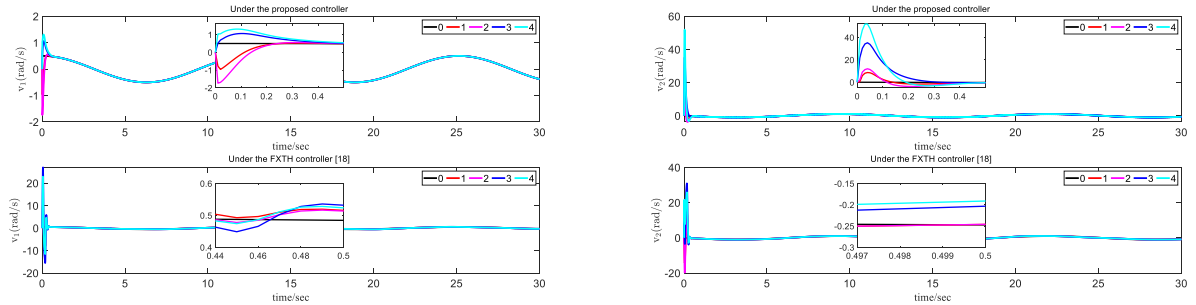

FIGURE 16. Angular velocity tracking effect comparison graph.

while avoiding the unnecessary jitter vibration phenomenon of the controller. The performance function constrains the angle error of the RMs to achieve the desired performance requirements. Filter is introduced to select signals at specific frequencies to improve the reliability of signal transmission. The proposed leader observer simulates the real-time monitoring of a given reference trajectory in an industrial environment to ensure the normal operation of multiple RMs under real working conditions. Finally, virtual simulations are performed by simulating sinusoidal function inputs to verify the effectiveness of the control strategy proposed in this paper.

The angle and angular velocity tracking of the multi-RMs are shown in Figs. 3 and 6, respectively. The tracking errors of the angle and angular velocity of the multiple RMs are shown in Figs. 7 and 8, in which the angular and angular velocity tracking errors can converge within a certain range under the action of the designed novel prescribed performance, the performance function is universal, and there is no obvious jitter in the errors. The filtering error and adaptive rate of

TABLE 2. Multi-RMs for the angle error of joint 1.

i	The proposed controller (rad)	The FXTH controller (rad)
1	-0.0005784	0.03274
2	-0.001157	0.02821
3	-002311	0.04154
4	-0.004486	0.03718

TABLE 3. Multi-RMs for the angle error of joint 2.

i	The proposed controller (rad)	The FXTH controller (rad)
1	0.000539	-0.05712
2	0.00117	-0.04903
3	0.001303	-0.07624
4	0.002597	-0.06852

TABLE 4. Multi-RMs for angular velocity error of joint 1.

i	The proposed controller (rad/s)	The FXTH controller (rad/s)
1	0.008015	0.03126
2	0.01568	0.02917
3	0.03148	0.04738
4	0.005768	0.03907

TABLE 5. Multi-RMs for angular velocity error of joint 2.

i	The proposed controller (rad/s)	The FXTH controller (rad/s)
1	-0.000401	0.00126
2	-0.0009193	0.001339
3	-0.008347	0.04398
4	-0.01751	0.05614

the prescribed time adaptive command filter are shown in Figs. 9 and 10, from which it is easy to see that the filtering error significantly overshoots in the initial stage and finally converges to the zero-value region quickly within the prescribed time. The quantized control input of the system and its partial enlargement are shown in Fig. 11. The angular and angular velocity and angular acceleration tracking errors of the prescribed time state observer are shown in Figs. 12-14. In addition, the multi-RMs angular and angular velocity following based on two different asymmetric Lyapunov barrier function cases are also given in Figs. 15-16. The comparative experiments of the multi-RMs of angular and angular velocity errors at $t = 0.5$ s under different controllers are given in Table 2-5, which show that the errors are smaller and the controller is clearly superior under the proposed prescribed time H_∞ controller.

V. CONCLUSION

In this paper, a prescribed time-adaptive H_∞ cooperative controller based on the log-type barrier Lyapunov function is proposed for multi-RM systems. The proposed novel prescribed performance ensures that the system achieves maximized performance while allowing the angle steady-state error to converge to a certain range in prescribed time. The ''complexity explosion'' problem is addressed by designing a prescribed time adaptive command filter. The prescribed time observer allows obtaining leader state information without acceleration measurements. In addition, an input quantization technique is introduced, which solves the problem of limited channel bandwidth of multi-RM systems in practical applications by converting continuous signals into segmented constant signals to reduce the communication rate. The proposed controller ensures that the multi-RM systems have prescribed time stability in the sense of bounded signals while avoiding the jitter problem. To prove the validity of these results, several examples of MRMS simulations are presented.

REFERENCES

[1] M. A. Chowdhury, S. S. S. Al-Wahaibi, and Q. Lu, ''Entropy-maximizing TD3-based reinforcement learning for adaptive PID control of dynamical systems,'' *Comput. Chem. Eng.*, vol. 178, Oct. 2023, Art. no. 108393.

[2] S. Niu, J. Wang, J. Zhao, and W. Shen, ''Neural network-based finite-time command-filtered adaptive backstepping control of electro-hydraulic servo system with a three-stage valve,'' *ISA Trans.*, vol. 144, pp. 419–435, Jan. 2024.

[3] Y. Hu, W. Liu, and B. Ma, ''Event-trigger-based composite adaptive fuzzy control for nonlinear time-varying state constraint systems with asymmetric input saturation,'' *Eur. J. Control*, vol. 75, Jan. 2024, Art. no. 100892.

[4] J. Fei, Y. Chen, L. Liu, and Y. Fang, ''Fuzzy multiple hidden layer recurrent neural control of nonlinear system using terminal sliding-mode controller,'' *IEEE Trans. Cybern.*, vol. 52, no. 9, pp. 9519–9534, Sep. 2022.

[5] S. Li, Y. Zhu, J. Bai, and G. Guo, ''Dynamic obstacle avoidance of unmanned ship based on event-triggered adaptive nonlinear model predictive control,'' *Ocean Eng.*, vol. 286, Oct. 2023, Art. no. 115626.

[6] H. Jahanshahi, Q. Yao, M. I. Khan, and I. Moroz, ''Unified neural output-constrained control for space manipulator using tan-type barrier Lyapunov function,'' *Adv. Space Res.*, vol. 71, no. 9, pp. 3712–3722, May 2023.

[7] Z. Xu and L. Zhao, ''Distributed adaptive gain-varying finite-time event-triggered control for multiple robot manipulators with disturbances,'' *IEEE Trans. Ind. Informat.*, vol. 19, no. 9, pp. 9302–9313, Sep. 2023.

[8] M. Li, J. Zhang, S. Li, and F. Wu, ''Adaptive finite-time fault-tolerant control for the full-state-constrained robotic manipulator with novel given performance,'' *Eng. Appl. Artif. Intell.*, vol. 125, Oct. 2023, Art. no. 106650.

[9] P. Yang, Y. Su, and L. Zhang, ''Proximate fixed-time fault-tolerant tracking control for robot manipulators with prescribed performance,'' *Automatica*, vol. 157, Nov. 2023, Art. no. 111262.

[10] D.-D. Zheng, X. Li, X. Ren, and J. Na, ''Intelligent control for robotic manipulator with adaptive learning rate and variable prescribed performance boundaries,'' *J. Franklin Inst.*, vol. 360, no. 11, pp. 7037–7062, Jul. 2023.

[11] Y. Sun, Y. Zhang, H. Qin, L. Ouyang, and R. Jing, ''Predefined-time prescribed performance control for AUV with improved performance function and error transformation,'' *Ocean Eng.*, vol. 281, Aug. 2023, Art. no. 114817.

[12] S. J. Yoo and B. S. Park, ''A universal error transformation strategy for distributed event-triggered formation tracking of pure-feedback nonlinear multiagent systems with communication and avoidance ranges,'' *Appl. Math. Comput.*, vol. 433, Nov. 2022, Art. no. 127412.

[13] A.-M. Zou, Y. Liu, Z.-G. Hou, and Z. Hu, ''Practical predefined-time output-feedback consensus tracking control for multiagent systems,'' *IEEE Trans. Cybern.*, vol. 53, no. 8, pp. 5311–5322, Oct. 2023.

[14] X. Liang, H. Wang, Y.-H. Liu, W. Chen, and T. Liu, ''Formation control of nonholonomic mobile robots without position and velocity measurements,'' *IEEE Trans. Robot.*, vol. 34, no. 2, pp. 434–446, Apr. 2018.

[15] Y. Zhao and X. Li, ''Observer-based event-triggered sliding mode control for delayed systems with unknown disturbances,'' *J. Franklin Inst.*, vol. 360, no. 13, pp. 10064–10079, Sep. 2023.

[16] R. Hao, H. Wang, M. Zhou, and W. Zheng, ''Distributed adaptive command filtered resilient event-triggered secure consensus control for multiagent systems under double DoS attacks,'' *Expert Syst. Appl.*, vol. 224, Aug. 2023, Art. no. 120016.

[17] H. Liu, X. Tian, G. Wang, and T. Zhang, ''Finite-time H_∞ control for high-precision tracking in robotic manipulators using backstepping control,'' *IEEE Trans. Ind. Electron.*, vol. 63, no. 9, pp. 5501–5513, Sep. 2016.

[18] Z. Wang, X. Tian, Q. Mai, and H. Liu, ''Fixed-time composite robust H_∞ tracking control of marine surface vessels based on the barrier Lyapunov function and an event-triggered strategy,'' *Ocean Eng.*, vol. 261, Oct. 2022, Art. no. 112113.

[19] H. Liu, Y. Li, X. Tian, and Q. Mai, ''Event-triggered predefined-time H_∞ formation control for multiple underactuated surface vessels with error constraints and input quantization,'' *Ocean Eng.*, vol. 277, Jun. 2023, Art. no. 114294.

[20] P. N. N. Thanh and H. P. H. Anh, ''Advanced neural control technique for autonomous underwater vehicles using modified integral barrier Lyapunov function,'' *Ocean Eng.*, vol. 266, Dec. 2022, Art. no. 112842.

[21] J. Liu, M. Zhao, and L. Qiao, ''Adaptive barrier Lyapunov function-based obstacle avoidance control for an autonomous underwater vehicle with multiple static and moving obstacles,'' *Ocean Eng.*, vol. 243, Jan. 2022, Art. no. 110303.

[22] S. Chen, Q. An, H. Zhou, and H. Su, ''Observer-based consensus for fractional-order multi-agent systems with positive constraint,'' *Neurocomputing*, vol. 501, pp. 489–498, Aug. 2022.

[23] J. A. V. Trejo, J.-C. Ponsart, M. Adam-Medina, G. Valencia-Palomo, J. A. V. Trejo, and D. Theilliol, "Distributed observer-based fault-tolerant leader-following control of multi-agent systems," *IFAC-PapersOnLine*, vol. 55, no. 6, pp. 691–697, 2022.
[24] S.-Y. Wei and Y.-X. Li, "Finite-time adaptive neural network command filtered controller design for nonlinear system with time-varying full-state constraints and input quantization," *Inf. Sci.*, vol. 613, pp. 871–887, Oct. 2022.
[25] R. Hao, H. Wang, and W. Zheng, "Dynamic event-triggered adaptive command filtered control for nonlinear multi-agent systems with input saturation and disturbances," *ISA Trans.*, vol. 130, pp. 104–120, Nov. 2022.
[26] S. Naha and D. K. Das, "Radial basis function neural network controller for power control of molten salt breeder reactor of nuclear power plant," *Ann. Nucl. Energy*, vol. 195, Jan. 2024, Art. no. 110160.
[27] K. Zhang, W. Hao, X. Yu, and T. Shao, "An interpretable image classification model combining a fuzzy neural network with a variational autoencoder inspired by the human brain," *Inf. Sci.*, vol. 661, Mar. 2024, Art. no. 119885.
[28] L. Wang and C. L. P. Chen, "Reduced-order observer-based dynamic event-triggered adaptive NN control for stochastic nonlinear systems subject to unknown input saturation," *IEEE Trans. Neural Netw. Learn. Syst.*, vol. 32, no. 4, pp. 1678–1690, Apr. 2021.
[29] L. Dai, X. Chen, L. Guo, J. Zhang, and J. Chen, "Prescribed-time group consensus for multiagent system based on a distributed observer approach," *Int. J. Control, Autom. Syst.*, vol. 20, no. 10, pp. 3129–3137, Oct. 2022.
[30] H. Yang and D. Ye, "Adaptive fixed-time bipartite tracking consensus control for unknown nonlinear multi-agent systems: An information classification mechanism," *Inf. Sci.*, vol. 459, pp. 238–254, Aug. 2018.
[31] Z. Chen, Q. Chen, X. He, and M. Sun, "Adaptive backstepping control design for uncertain rigid spacecraft with both input and output constraints," *IEEE Access*, vol. 6, pp. 60776–60789, 2018.
[32] W. Guo, L. Wang, L. Shi, W. Sun, and H. Jahanshahi, "Predefined-time stability for a class of dynamical systems and its application on the consensus control for nonlinear multi-agent systems," *Inf. Sci.*, vol. 626, pp. 180–203, May 2023.
[33] C. Wang, Y. Wu, F. Wang, and Y. Zhao, "TABLF-based adaptive control for uncertain nonlinear systems with time-varying asymmetric full-state constraints," *Int. J. Control*, vol. 94, no. 5, pp. 1238–1246, May 2021.
[34] X. Zhang, Z. H. Zhu, S. Xie, H. Gao, and G. Li, "Barrier function-based prescribed-performance adaptive attitude tracking control for spacecraft with uncertainties," *J. Franklin Inst.*, vol. 360, no. 12, pp. 8075–8095, Aug. 2023.
[35] Z. Xu, Q. Liu, and J. Yao, "Funnel function-based adaptive prescribed performance output feedback control of hydraulic systems with disturbance observers," *ISA Trans.*, vol. 136, pp. 701–714, May 2023.
[36] Y. Zhang, G. Wu, X. Yang, and S. Song, "Appointed-time prescribed performance control for 6-DOF spacecraft rendezvous and docking operations under input saturation," *Aerosp. Sci. Technol.*, vol. 128, Sep. 2022, Art. no. 107744.
[37] H. Liu, B. Meng, and X. Tian, "Finite-time prescribed performance trajectory tracking control for underactuated autonomous underwater vehicles based on a tan-type barrier Lyapunov function," *IEEE Access*, vol. 10, pp. 53664–53675, 2022.
[38] B. Xu, Y. Liang, Y.-X. Li, and Z. Hou, "Adaptive command filtered fixed-time control of nonlinear systems with input quantization," *Appl. Math. Comput.*, vol. 427, Aug. 2022, Art. no. 127186.
[39] X. Liu, C. Qiu, Q. Zeng, A. Li, and N. Xie, "Time-energy optimal trajectory planning for collaborative welding robot with multiple manipulators," *Proc. Manuf.*, vol. 43, pp. 527–534, Jan. 2020.
[40] Q. Yu, G. Wang, X. Hua, S. Zhang, L. Song, J. Zhang, and K. Chen, "Base position optimization for mobile painting robot manipulators with multiple constraints," *Robot. Comput.-Integr. Manuf.*, vol. 54, pp. 56–64, Dec. 2018.

WEICHEN LI received the B.E. degree from Linyi University, China, in 2022. He is currently pursuing the master's degree with the School of Mechanical Engineering, Guangdong Ocean University, China. His research interests include multiagent systems and robust adaptive control.

HAITAO LIU (Member, IEEE) received the Ph.D. degree from the School of Mechanical and Automotive Engineering, South China University of Technology, Guangzhou, China, in 2012. He is currently a Professor with the School of Mechanical Engineering, Guangdong Ocean University, Zhanjiang, China. His research interests include the theory and applications of nonlinear control and robotics.

XUEHONG TIAN received the M.S. degree in mechanical engineering from Guangdong Ocean University, Zhanjiang, China, in 2018. She is currently an Associate Professor with the School of Mechanical Engineering, Guangdong Ocean University. Her research interests include robot control, multiagent systems, and nonlinear system design.